Defence Science Journal, Vol. 71, No. 5, September 2021, pp. 581-587, DOI : 10.14429/dsj.71.16699

An Iterative Approach towards Single-stage Axial Fan Design using Off Design Prediction

Rajat Arora*, Ramraj H. Sundararaj, and Abhijit Kushari

Department of Aerospace Engineering, Indian Institute of Technology Kanpur Kanpur - 208 016, India
**E-mail: rajatar@iitk.ac.in*

ABSTRACT

A single-stage axial fan having a pressure ratio of 1.01 is designed in the current study. The design pressure ratio is chosen based on the power available from the existing motor (2.2 kW). The design space for the axial flow fan was generated by varying specific flow and geometrical parameters in suitable steps, using a program written in MATLAB. The varied flow parameters are mass flow rate, inlet Mach number, inlet flow angle, and rotor speed. The geometrical parameters that were varied are hub to tip ratio, aspect ratio, and blade solidity. Using these as the input variables and applying free vortex theory for 3-dimensional blade design, the aerodynamic design of the axial flow fan was carried out. Performance parameters like flow coefficient, stage loading coefficient, degree of reaction, diffusion factor, De Haller's number, and blade angles were calculated at the blade's hub, mean, and tip. Total design space of 92160 data points was obtained from the combination of input parameters. Several constraints were applied to optimise the design space based on the available power from the existing motor and in-house manufacturing limitations. The initial design space was reduced to 82 data points using these constraints. To further reduce the number of points in the design space, off-design performance was evaluated for each of these data points. Following this, one design point was selected based on the optimum performance range in off-design operation, while considering manufacturing limitations. Using Mellor charts, a suitable blade profile was chosen based on the inlet and exit blade angles. NACA 65-410 airfoil was selected with a stagger of 55 degrees and an incidence of 6 degrees for optimum performance.

Keywords: Axial flow fan; Turbomachines; Off-design performance; Cascade; NACA-65410; Surge margin

NOMENCLATURE

A	Annulus Area (m^2)
AR	Aspect Ratio
B	Number of blades
C	Absolute velocity at D_m (m/s)
C_P	Specific heat at constant pressure J/kg-K
D	Diameter (m)
DF	Diffusion Factor
D_h/D_t	Hub-tip ratio
H	Blade height (m)
$\dot{m}$	Mass flow rate of air (kg/s)
M_a	Inlet axial Mach number
N	Rotor speed in Revolutions per minute
P	Pressure (Pa)
$\dot{P}$	Power or Compressor work/s (kW)
ΔP	Desired pressure rise (Pa)
R	Degree of reaction
R_e	Reynolds number based on W_1
R_{gas}	Specific gas constant J/kg-K
T	Temperature (K)
S	Solidity
SM	Surge margin
W	Relative velocity at D_m (m/s)
c	Chord length (m)
i	Incidence angle (degree)
α	Absolute air angle at D_m (degree)
β	Relative air angle at D_m(degree)
θ_2	Blade momentum thickness
η	Isentropic efficiency in percentage
Y_p	Stagnation pressure loss coefficient
ϕ	Flow Coefficient
ψ	Stage loading coefficient
λ	Work done factor
χ	Twist in blade (degree)
γ	Ratio of specific heat
μ	Dynamic viscosity at 298 K(kg/s-m)
$\frac{C_{max,s}}{C_2}$	Diffusion ratio

Subscript

1	Entry to rotor
2	Exit of rotor (or) entry to stator
3	Exit of stator
0	Stagnation properties
d	Design point
ex	Expected
h	Hub
m	Mean
max	Maximum
min	Minimum
r	Rotor
s	Stator
t	Tip
tt	Total to total

Received : 28 January 2021, Revised : 26 May 2021
Accepted : 16 June 2021, Online published : 02 September 2021

1. INTRODUCTION

Axial fans find application preliminarily in supplying air for ventilation and industrial applications like HVAC, electrical appliances, and automobiles. Fans are supplied mechanical energy through a rotating shaft, the rotating fan blades then transmit this energy onto the air to generate sufficient pressure to move air overcoming the resistance developed by the ducts and other components installed in the fan system.

The axial fans are broadly categorised into three different types: propeller, tube axial and vane axial depending upon the flow rate created and static pressure developed. Propeller type is suited for high flow rate and low-pressure rise application but efficiencies are on the lower end. In contrast, tube axial fans are used for medium pressure rise capabilities and vane axial are equipped with guide vanes at the front or rear to recover the pressure and achieving higher efficiencies by removing swirl in the flow.

The design of vane axial fans was first discussed by Wallis[1] using the "isolated airfoil method" and "cascade airfoil method". The preceding method utilised lift data for designing whereas the latter was based on flow deflection obtained in cascades.

Defining blade cross-section forms the core of axial flow fan design. It consists of defining the blade chord, chord length, stagger angle, and camber angle. Hay[2], *et al.* compiled available data for a variety of airfoils and generated carpet plots. The plots contained information regarding the variation of lift coefficient with camber angle and incidence angle. These plots allowed the user to choose the operating regime far away from a stall region and has a higher lift to drag ratio. Bleier[3] has discussed the design methodology of vane axial fans; the hub to tip ratio lies in the range of 0.5 to 0.8 because of higher static pressure. The hub diameter is first selected based on the static pressure required. The dimension of tip diameter is further calculated based on the airflow rate and design speed of the fan. Carolous & Starzmann[4] integrated the existing blade element theory with isolated airfoil to assess different airfoil shapes better. Their research was limited to low-pressure airfoils as blade to blade interaction is considered negligible in isolated airfoil theory. Nonetheless, it indeed accounted for the actual Reynold's number, Mach number, and geometrical modifications. Castegnaro[5] compared the results from the modified cascade theory and modified isolated airfoil method. He further formulated a mixed approach that considers both these methods to design the medium solidity fans accurately.

Diverging from the traditional designing methods inverse cascade design method has become a popular method lately. Optimising the shape of the blade for a given operational regime leads to better performance. Huang & Gau[6] showed that redesigning the fan blades based on inverse technique increases flow rates as compared to design flow rates, thereby enhancing the performance of system. Angelini[7], *et al.* have stressed the fact that primary parameters such as specific speed and blade diameter have been employed for the fan design process over the years. Still, effect of secondary parameters like blade number or hub tip ratio is not explicitly used. The authors have attempted to use the design space available for 10,000 axial fans to develop correlations between design and performance features.

Even though various methods of designing a fan stage exist, the authors have attempted to consider all the possible variables that can impact fan performance in the design phase. The advantage of this approach is to eliminate the combinations of the input parameters that can degenerate the fan performance. The constraints applied to reach an optimal solution can be tweaked by the user based on the manufacturing limitations at least in educational institute laboratories. The analysis is limited to single-stage design in the current work, but it can be easily extended to a multistage design process if required.

The objective of this work is to develop a straightforward and rapid design methodology to design axial flow fans. A single-stage axial flow fan is designed using a conventional design approach involving mean-line analysis followed by three-dimensional design. The design involves an iterative procedure using multiple input parameters, which yielded multiple design point solutions. The design space was then suitably optimised by applying manufacturing and aerodynamic constraints. To further optimise the design space and converge upon fewer solutions, off-design analysis was carried out. The subsequent sections detail the design process involved and the ensuing analysis.

2. INPUT PARAMETERS

The initial parameters chosen for this design process are shown in Table 1. Typical axial flow fan efficiencies range between 75% to 85%. The higher end of this spectrum was chosen for this design, keeping the isentropic total-to-total efficiency at 85%.

Table 1. Input parameters that were kept constant during the design process

Constants	
Parameter	**Value**
P_{01}	101325 Pa
T_{01}	298 K
η	85%
ΔP_0	1,000 Pa
Y_{pr}	0.07
Y_{ps}	0.07
λ	1.03
C_P	1,005 J/kg-K
γ	1.4
R_{gas}	287 J/kg-K
μ	1.83 E-5 (kg/s-m)

For the initial design, multiple iterative parameters are selected. A wide range is chosen for all the iterative parameters, facilitating an ample design space consisting of all possible solutions. The loop count in Table 2 represents the number of times a given parameter is varied and is calculated by Eqn (1). The total number of iterations is a multiplication of loop counts of all the parameters that were iterated during the code.

$$L_k = \frac{Max - Min}{Stepsize} + 1 \quad (1)$$

Table 2. Parameters that were iterated to generate design space

Iteration parameters			
Parameter	**Range**	**Step size**	**Loop count (L_k)**
$\dot{m}$	0.5 – 2.5	0.5	5
M_a	0.1 – 0.3	0.1	3
α_1	0 – 60	10	7
N	2,000 – 16,000	2,000	8
D_h/D_t	0.3 – 0.7	0.1	5
AR	1 – 3	0.5	5
S_r	0.5 – 1.5	0.5	3

$$Iterations = L_{k1} \times L_{k2} \times L_{k3} \times L_{k4} \times L_{k5} \quad (2)$$

3. METHODOLOGY OF DESIGN

Using the parameters listed in the previous section, the iterative design process is carried out, using an in-house code in MATLAB. Preliminary design is carried out using a standard mean-line design approach[8,9]. The mean-line is assumed to be constant across the rotor and stator. Since the density variations are negligible, hub diameter and tip diameter further remain constant across the stage. The absolute air angles at the entry and the exit to the stage are kept the same during the calculations ($\alpha_1=\alpha_3$), following the repeating stage design procedure. Three-dimensional design is carried out using free vortex theory where work done remains the same at the radii and radial equilibrium is maintained with the assumption of axial velocity (C_a) remaining constant throughout the stage. The flow angles and velocities are calculated at the hub and tip as well in the manner depicted in Fig. 1.

4. OPTIMISATION OF DESIGN SPACE

Without applying any constraints, based on the number of parameters being iterated and their step size, we would have 63,000 design solutions. To optimise the design space and reduce the number of possible solutions, certain constraints were applied. The constraints are listed in Table 3 were applied. The compressor work was limited to 1.2 kW to use the existing spindle motor, with a rated output of 2.2 kW. The minimum hub diameter is set at 0.12 m, allowing the existing spindle motor to be mounted inside the hub. For facilitating the comparison of linear cascade data with the data acquired from the axial flow fan, Reynolds number similarity is maintained between the two. The Reynolds number based on chord for the linear cascade is ~1.4 x 10^5, which serves as the upper limit. Due to anticipated manufacturing constraints, blade twist is limited to 20 degrees for the rotor and stator and the chord length is maintained above 25 mm. Blade twist refers to the difference in inlet relative flow angle (β_1) at the hub and tip of the blade, as a result of applying free vortex condition for 3-D design. The other constraints concerning the machine's performance are the degree of reaction, flow coefficient, stage loading coefficient and diffusion factor. These performance-related constraints are applied at all locations, i.e. mean, hub and tip of the blade.

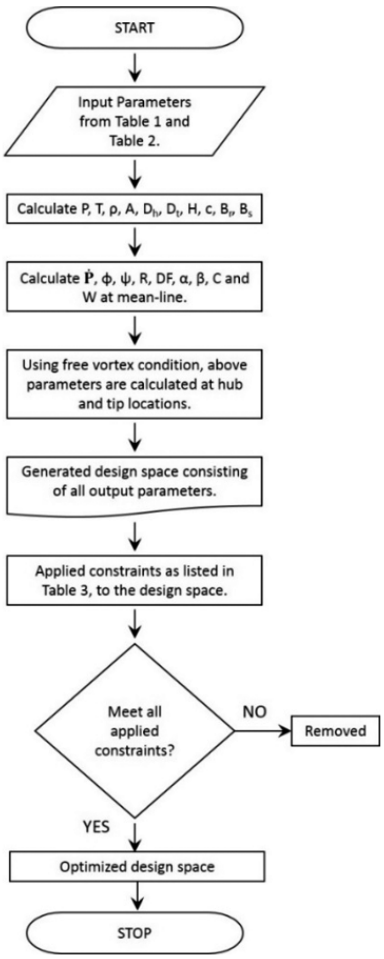

Figure 1. Design process flowchart.

Table 3. Constraints used for optimising design space

Constants	
Parameter	**Value**
$\dot{P}$	< 1.2 kW
R_e	1 x 10^5 – 1.4 x 10^5
D_h	> 0.12 m
χ	< 20°
c	> 0.025 m
R	0 – 1
ϕ	0.4 – 0.8
ψ	< 0.5
DF_r	0 – 0.6
B_s	< 20

Following the application of these constraints, the design space was reduced to 4 points. Even though a vast parameter space of 63,000 points was chosen, the final reduced design space contained a narrow range of results that satisfied all the applied constraints. All the feasible solutions collapsed into a narrow range, where the inlet Mach number, hub/tip ratio, aspect ratio, and solidity were constant. There were minor variations in inlet mass flow rate and rotor speed. The inlet air angle varied between 0 and 30 degrees. Due to the larger step size, many possible design solutions that were contained

within the iteration space were not explored. To further investigate the design space and check whether other possible solutions satisfying all the constraints existed, the range and the step size were reduced. This exercise could have been done on the initial range of iteration parameters, but it would have resulted in large amounts of data and longer processing times. To avoid this, the procedure was split into two parts, where the first iteration is used for coarse tuning of the design space, and the second iteration is used for fine-tuning the design space. The reduced range and the new step size for all the iteration parameters are shown in Table 4. An additional constraint was applied, which is ψ should be between 0.25 and 0.5 at the mean diameter.

Table 4. Revised range based on the initial design process

Iteration parameters with the new range			
Parameter	**Range**	**Step size**	**Loop count (L_k)**
$\dot{m}$	0.5 – 1.4	0.1	10
M_a	0.1 – 0.2	0.05	3
α_1	0 – 35	5	8
N	5000 – 16000	1000	12
D_h/D_t	0.58 – 0.7	0.04	4
AR	1 – 1.5	0.5	2
S_r	0.5 – 1.25	0.25	4

While the initial design iteration yielded only 4 out of the 63,000 available solutions, the second iteration using the reduced range and smaller step size yielded 82 out of the 92,160 available solutions. All 82 solutions met all the constraints outlined earlier. This was due to the smaller step size that was chosen during the iterative procedure, yielding more points within the reduced design space that met the requirements. This posed a new predicament, where all the 82 possible solutions were equally viable and each had its distinct advantages and disadvantages. To further down-select, the efficiency of the stage was calculated, based on the total pressure loss coefficient for the rotor and stator.

5. EXPECTED EFFICIENCY

The stage isentropic efficiency was assumed to be 85% at the start of the design process. This was kept constant for all the design iterations that were carried out thus far. The expected efficiency was calculated again using Eqn (3) given below:

$$\eta_{ttex} = 1 - \frac{0.5 Y_{pr} W_1^2 + Y_{ps} C_2^2}{C_p \left(T_{03} - T_{01}\right)} \tag{3}$$

At low Mach numbers, the total pressure loss coefficient is roughly 0.02 and remains fairly invariant for a wide range of incidences. The total pressure loss coefficient mentioned above is for a cascade, which is profile loss. In an axial flow fan, additional losses will be incurred due to secondary and 3-D flows. The magnitude of these losses is comparable to the profile loss. To account for these additional losses, the profile loss was increased by a factor of 3.5. Consequently, a loss coefficient of 0.07 is used for the rotor (Y_{pr}) and stator (Y_{ps}). The value of loss coefficient varies with a wide range of parameters like flow Incidence angle, blade stagger angle, solidity, Aspect ratio. The exact value should be determined experimentally or computationally for a selected blade profile. A reasonable estimate of two-dimensional loss coefficient is given by Eqn (4). The loss coefficient given by Eqn (4), considers the inlet and exit flow angles, blade solidity, and the ratio of wake momentum thickness to chord. The ratio of momentum thickness to chord given by Eqn (5) depends upon the diffusion ratio, which in turn depends upon the flow angles and solidity. It is to be pointed out that while estimating the loss coefficient for a rotor, the inlet flow angle α_1 should be replaced with β_1, and exit flow angle α_2 is to be replaced with β_2 in the Eqns (4-6). However, at this juncture, a loss coefficient of 0.07 is used to compare the multiple design options. The expected efficiency ranged between 76% and 82% for all 82 cases. The code can be clubbed with the available experimental data in the literature to improve the accuracy.

$$Y_p = 2\left(\frac{\theta_2}{c}\right)\left(\frac{c}{s}\right)\frac{\cos^2\alpha_1}{\cos^3\alpha_2} \tag{4}$$

$$\frac{\theta_2}{c} = \frac{0.04}{\left\{1 - 1.17\ln\left(\frac{C_{\max,s}}{C_2}\right)\right\}} \tag{5}$$

$$\frac{C_{\max,s}}{C_2} = \frac{\cos\alpha_2}{\cos\alpha_1}\left[1.12 + 0.61\left(\frac{s}{c}\right)\cos^2\alpha_1\left(\tan\alpha_1 - \tan\alpha_2\right)\right] \tag{6}$$

At this juncture, it should have been a simple matter of choosing the design point with the highest expected efficiency as the final design solution for this exercise. The design point for maximum efficiency yields a 54% reaction at the mean diameter, usually considered ideal. However, this design point also has the maximum blade twist for rotor and stator, highest blade count, and requires the use of IGV's. Even though they meet the previously set constraints for blade twist and blade count, a lower twist and lower blade count are always desired for manufacturing simplicity. The design with the least blade twist or minimum blade count has a much lower expected efficiency, which is also not desirable. To improve the process of selecting a single design that is best suited, an off-design analysis was carried out, as detailed in the subsequent section.

6. OFF-DESIGN PERFORMANCE

It is critical for a compressor stage to operate at conditions away from the operating point; hence it must be capable of operating reasonably well over a wide range of inlet conditions and rotational speeds. After applying the constraints, off-design performance was evaluated for the 82 cases obtained in the second design iteration.

For a compressor operating at a constant rotational speed, changes in mass flow rate will move its operation to off-design. If the mass flow is reduced, the incidence onto the blades increases, and the stage moves toward an unstable operating regime. At an increased mass flow, the incidence decreases becoming negative, and the blade passages may choke. For

a low-speed compressor, the operation is independent of rotational speed, and there is no risk of the flow choking[10]. The performance characteristic can be presented as a single curve relating stage loading ψ to flow coefficient ϕ. Howell predicted the method to evaluate the off-design performance of a low-speed compressor stage based on the cascade experiments conducted by Horlock, where his results showed that α_1 and β_2 do not change substantially over a range of incidences[10]. The above assumption neglects any variations in flow deviation. The simplified expression for evaluating off-design performance is given by Eqn (7).

$$\psi = 1 - t\phi \tag{7}$$

$$t = \tan\alpha_1 + \tan\alpha_2 = Constant \tag{8}$$

$$t = \frac{1 - \psi_{design}}{\phi_{design}} \tag{9}$$

$$SM = \left(\frac{\psi_{\max} - \psi_{design}}{\psi_{design}} \right) \times 100 \tag{10}$$

The value of t can be obtained by Eqn (9), implying that t has a unique value for a given ψ_d and ϕ_d. Off-design performance maps were generated for the mean line by varying flow coefficient from 0.5 times of ϕ_d to 1.25 times of ϕ_d in steps of 0.005, whereas N, α_1 and β_2 were kept at the design value. The range for flow coefficient was chosen keeping in mind that it should not exceed 1 or go below 0.2, which is just exceeding the previously applied constraint of 0.4 – 0.8. Stage loading coefficient was calculated by using Eqn (7). For a given value of ϕ and ψ other parameters like β, α, C, W, and DF_r were calculated. The diffusion number at the mean was constrained between 0.15-0.45, to get the upper and the lower limits of the performance map. Surge margin was then calculated using Eqn (10).

A typical off-design map for one such combination of ψ_d and ϕ_d is shown in Fig. 2. Similar calculations were repeated for all 82 cases and surge margin was calculated. Further truncation of the optimised 82 cases was done based on the surge margin. The design points that had a higher efficiency had a surge margin of less than 10%. The final design point was selected considering that a high surge margin, expected efficiency, and blade height were desired with a lower blade twist and blade count.

The input parameters along with the calculated parameters are shown in Table 5. The maximum and minimum incidence, for which DF_r was within the range, is also shown in this table. The velocity triangle, shown in Fig. 3, represents the velocities at the inlet and exit for this design, along with the flow angles. This final design point offered the maximum blade height, largest surge margin and had an even distribution of positive and negative incidences. Some of the other designs that offered a similar blade height and surge margin, did not have an even distribution of positive and negative incidences. However, the final selected design point has lower estimated efficiency and a higher reaction at the mean when compared to many other cases.

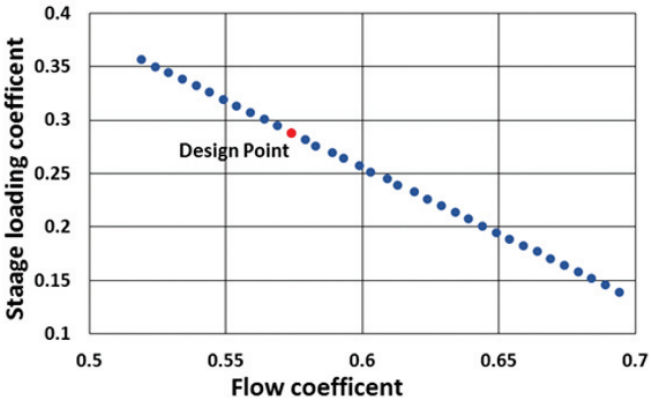

Figure 2. Off-design compressor map in terms of ϕ and ψ.

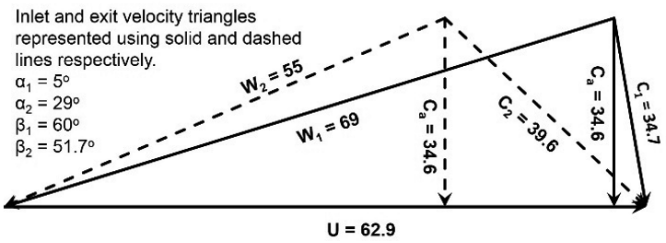

Figure 3. Inlet and exit velocity triangles for the selected design point.

Table 5. Selected design point parameters

Input parameters						
$\dot{m}$	M	α_1	N	D_h/D_t	AR	S_r
1	0.1	5	7000	0.58	1.5	1
Geometric design parameters						
D_t	D_h	B_r	B_s	Re	$\dot{P}$	χ
0.22	0.13	18	19	1.35	1.02	15
Aero-thermodynamic design parameters						
R	ϕ	ψ	D	$\eta_{tt\ ex}$	SM	i_{max} to i_{min}
0.82	0.55	0.26	0.31	77.6%	36%	3.4° to -4.1°

7. BLADE PROFILE SELECTION

The highest relative Mach number that these blades will be subjected to is less than 0.3. Hence, NACA 65 series airfoil, circular arc or parabolic arc blade profiles can be used[11]. To determine a suitable blade profile, available cascade data for NACA 65 series blade profiles are used[12]. For selected geometries at various staggers and incidence angles, the deflection angle, total pressure loss, and blade pressure surface pressure distributions are available. To make this data easier to use for design purposes, they were converted into various carpet plots[13]. From the design process detailed in the previous sections, inlet air angle, flow turning angle, inlet Mach number, and solidity are known. Using this information along with the carpet plots, we can determine the blade camber angle, design angle of attack, and pressure rise coefficient. We can also use these charts to determine the off-design variation in the angle of attack and flow turning angle. Mellor[14], replotted these multiple

carpet plots in a more straightforward form, commonly referred to as Mellor charts. An example of a Mellor chart is shown in Fig. 4, with the inlet and exit flow angles on the X-axis and Y-axis respectively. The dark lines that form the boundary are incidence angles at which the drag coefficient becomes 50% more than the mean unstalled drag coefficient.

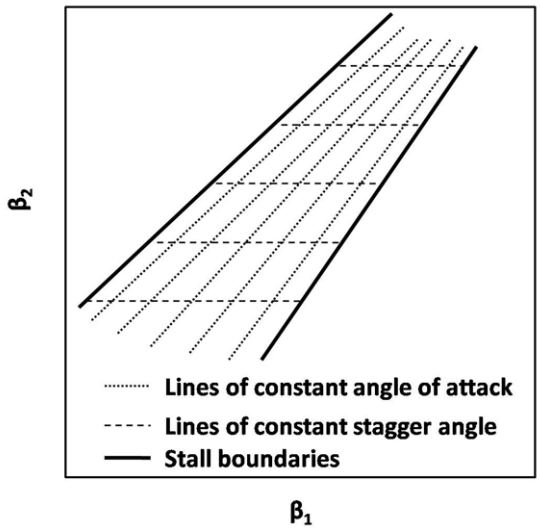

Figure 4. Characteristic representation of cascade data using Mellor's chart.

For an inlet relative flow angle of 60°, an exit relative flow angle of 51.7° and solidity of 1, various profiles were considered using Mellor charts. NACA 65-410 was selected since the point of intersection for these parameters was at the center of the region bounded between the two dark boundary lines, as shown by estimated i_{max} and i_{min} in Table 5. The design incidence angle was 6° and the stagger angle was 55°, from the Mellor chart for NACA 65-410. This value was close to the calculated stagger angle and design incidence angle based on the selected design point. On similar lines, for an inlet flow angle of 29° and exit flow angle of 5°, NACA 65-(18)10 profile was chosen for the stator, using Mellor charts. The design incidence angle is 10° and the design stagger angle is 20° for the stator.

8. CONCLUSION

The design of an axial flow fan was presented considering input parameters. These were iterated over a range with a suitable step size, for generating the design space. The initial design space had 63,000 data points. Constraints were applied to this design space to reduce the number of data points. The design space that resulted after the application of these constraints had only 4 design points. All these design points converged onto a small range of input parameters.

To further investigate this design space, the input parameters range was reduced and step size suitably altered. Applying constraints to the new range yielded 82 possible design points. Expected efficiency was calculated using a representative value of rotor and stator losses to further reduce the number of points. The expected efficiency was highest for cases with maximum rotor twist, blade count and required IGV's. If a design point with the least twist and blade count was chosen, the expected efficiency was much lower. To add another dimension to the selection process, off-design performance was evaluated for all 82 design points.

Off-design performance was evaluated at a constant rotational speed, by varying the flow coefficient. The off-design performance was assessed under the assumption that there is minimal or no change in inlet flow angle and exit relative flow angle over a wide range of incidences. Surge margin was also calculated for all the design points. It was seen that the design point with the highest expected efficiency also had the lowest surge margin, while the design with the most significant surge margin had a much lower efficiency. The final design point was chosen based on a compromise between surge margin, efficiency, blade twist, blade height, and blade count.

Based on the inlet and exit flow angles for the selected design point, the blade profile was chosen using Mellor charts. The final blade profile that was selected at the mean line was NACA 65-410 for the rotor and NACA 65-(18)10 for the stator. The code developed can be further modified to design multiple stages for axial compressor studies.

REFERENCES

1. Wallis, R.A. Axial flow fans-Design and Practice. Academic Press New York, London,1961.
2. Hay, N.; Metcalfe, R.; & Reizes, J.A. A Simple Method for the Selection of Axial Fan Blade Profiles. *Proc. of the Ins. of Mech. Eng*., 1978, **192**(1), 269-275. doi:10.1243/PIME_PROC_1978_192_028_02
3. Bleier, F.P. Fan Handbook- Selection, Application and Design. McGraw Hill Publication, 1997.
4. Carolus, T.H.; & Starzmann, R. An Aerodynamic Design Methodology for Low Pressure Axial Fans With Integrated Airfoil Polar Prediction. *In* Proc. of the ASME Turbo Expo 2011: Turbine Technical Conference and Exposition. Volume 4: Cycle Innovations; Fans and Blowers; Industrial and Cogeneration; Manufacturing Materials and Metallurgy; Marine; Oil and Gas Applications GT2011-45243, June 6–10, 2011, Vancouver, British Columbia, Canada doi: 10.1115/GT2011-45243
5. Castegnaro, S.; Fan Blade Design Methods: Cascade Versus Isolated Airfoil Approach-Experimental and Numerical Comparison. *In* Proc. of the ASME Turbo Expo 2016: Turbomachinery Technical Conference and Exposition. Volume 1: Aircraft Engine; Fans and Blowers; Marine GT2016-56994, V001T09A007, June 13–17, 2016, Seoul, South Korea. doi:10.1115/GT2016-56994
6. Huang, CH.; & Gau, CW. An optimal design for axial-flow fan blade: theoretical and experimental studies. *J Mech. Sci. Technol*., 2012, **26**(2), 427–436. doi: 10.1007/s12206-011-1030-7
7. Angelini, G.; Corsini, A.; Delibra, G. & Tieghi, L. Exploration of Axial fan Design Space with Data Driven Approach. *Int. J. Turbomach. Propuls. Power*., 2019, **4**(2), 11. doi: 10.3390/ijtpp4020011

8. Cohen, H.; Rogers, G.F.C. & S.H.I. Gas Turbine Theory. Longman group Limited, 1996.
9. Cumpsty, N.A. Compressor Aerodynamics. Longman group Limited, 1989.
10. Dixon, S. & Hall, C. Fluid Mechanics and Thermodynamics of Turbomachinery, Butterworth-Heinemann, 2014.
11. Wright, L.C. Blade Selection for a Modern Axial-Flow Compressor. *In* Fluid Mech., Acoustic, and Des. Of Turbomach., Part II, pp. 603–626,1970.
12. Herrig, B. L. J.; Emery, J. C. & Erwin, J. R. Systematic Two-Dimensional Cascade Tests of NACA 65-Series Compressor Blades at Low Speeds. NACA Research Memorandum, Sept. 1951.
13. Felix, R. Summary of 65-Series Compressor-Blade Low-Speed Cascade Data by Use of the Carpet-Plotting Technique, NACA Technical notes, July,1958.
14. Horlock, J. Axial Flow Compressors. Butterworths Scientific Publications, London, 1958.

ACKNOWLEDGEMENTS

The authors would like to thanks Mr T. Chandrasekar for his constant suggestions and comments that significantly improved the manuscript.

CONTRIBUTORS

Mr Rajat Arora is an Associate Member of the Aeronautical Society of India (AMAeSI). He did his Master's in Aerospace Propulsion from IIST Trivandrum. He is currently working as a PhD student at IIT Kanpur. His research interest includes Turbo-machines, Gas-turbines, and Aero-acoustics.
In the current article, he has proposed the course of action and built the in-house code for axial fan design.

Mr Ramraj H. Sundararaj has done BE in Aeronautical Engineering from the University of Madras and MSc in Gas Turbine Engineering from Cranfield University. He is working in the turbomachinery domain as a PhD scholar at IIT Kanpur. His topics of curiosity are gas turbine performance, combustion diagnostics, and compressible flows.
In the current research, he has put forth the suggestion of selection of airfoil based on the off-design performance.

Dr Abhijit Kushari received his PhD from Georgia Institute of Technology, Atlanta, Georgia, USA. Presently he is working as Head of the Department of Aerospace Engineering, IIT Kanpur. His research interest includes Rocket and Gas turbine propulsion, flow physics and flow control, fluid-structure interaction, Fire dynamics and suppression, and Aero-acoustics.
In this research article, he has provided valuable inputs regarding the optimisation of design space and thoroughly scrutinised the manuscript to reach the present form.